JPE 19-4-3

https://doi.org/10.6113/JPE.2019.19.4.858
ISSN(Print): 1598-2092 / ISSN(Online): 2093-4718

Analysis, Design and Implementation of Flexible Interlaced Converter for Lithium Battery Active Balancing in Electric Vehicles

Shuailong Dai*, Jiayu Wang*, Teng Li*, Zhifei Shan*, and Yewen Wei†

*College of Electrical Engineering and New Energy, China Three Gorges University, Yichang, China
†Hubei Province Collaborative Innovation Center for New Energy Microgrids,
China Three Gorges University, Yichang, China

Abstract

With the widespread use of modern clean energy, lithium-ion batteries have become essential as a more reliable energy storage component in the energy Internet. However, due to the difference in monomers, some of the battery over-charge or over-discharge in battery packs restrict their use. Therefore, a novel multiphase interleaved converter for reducing the inconsistencies of the individual cells in a battery pack is proposed in this paper. Based on the multiphase converter branches connected to each lithium battery, this circuit realizes energy transferred from any cell(s) to any other cell(s) complementarily. This flexible interlaced converter is composed of an improved bi-directional Buck-Boost circuit that is presented with its own available control method. A simulation model based on the PNGV model of fundamental equalization is built with four cells in PSIM. Simulation and experimental results demonstrate that converter and its control achieve simple and fast equalization. Furthermore, a comparison of traditional methods and the HNFABC equalization is provided to show the performance of the converter and the control of lithium-based battery stacks.

Key words: Battery energy storage, Bidirectional equalization, Flexible interlaced converter, PNGV model

I. INTRODUCTION

With the construction of China's smart grid, new energy vehicles have been being extensively used due to their environmental friendliness, loading controllability and close coordination with aggregators and charging stations [1]-[3]. As a source of power for new energy vehicles, battery cells are of vital importance in terms of power character [4]-[7]. Consequently, various equilibrium circuit topologies with control methods have been designed to decrease the hazards of battery pack inconsistencies [8]-[14].

In [8], a dual-input high step-up DC/DC converter with zero voltage turn-off (ZVT) is proposed to improve the efficiency of the converter using soft-switching techniques. Then with the increase of the power supply unit, the control complexity will be significantly increased, which will cause difficulties in engineering. In [9], a modular equilibrium system was proposed, which contain N cells and M equalizers. The deficiencies of this implementation lie in the complexity of its circuit structure and an unavoidable process to reach the primary balance by adjusting the states of twelve switching tubes. In [10], the topology of a time-sharing flyback converter is proposed, where any of the single cells in the battery stack can be equalized. Each cell shares one equalization module in the control gap of a low-power microcontroller. The transformer is applied to this topology, which limits the volume and weight of the converter to some extent. A novel switching circuit that requires none voltage estimation is proposed [11]. With a single-charge equalizer based on a multi-winding transformer, the energy transformed in a battery pack is delivered by the magnetic circuit of the multi-winding transformer, which inevitably leads to a huge quantity

Manuscript received Oct. 17, 2018; accepted Apr. 1, 2019
Recommended for publication by Associate Editor Huiqing Wen.
†Corresponding Author: weiyewen8@126.com
Tel: +86-137-7419-8153, Fax:+86-639-2170, China Three Gorges University
*College of Electrical Engineering & New Energy, China Three Gorges University, China

of magnetic loss. In [12], an innovative method of energy sharing control scheme was adopted to self-adapt the rate of charging for all of the cells, which fundamentally eliminates the difference in the state of charge (SOC) among batteries. Choosing a lossless DC power converter results in reaching equilibrium slowly. In [13], fast equalization was realized by a buck converter with an Adaptive Unscented Kalman (AUK) filter for SOC Estimation. When compared with traditional methods, its advantages include a simplified circuit structure, reduced energy loss and a fast response. The experiment only performed four cell balancing, which is difficult to expand and apply in large-scale series battery balancing. One approach to expanding the battery string scale is the use of natural equalization [14]-[16], where energy naturally flows to the cells and measuring sensor equipment is not required.

The standard solution to this problem is based on the flexible control method of battery cells in this paper. The proposed control method is derived from natural equilibrium, which eliminates the shortcoming of the current decrease in the later equilibrium stage. Natural control makes energy flow naturally between overcharged batteries and other batteries with forced energy donors and acceptors. In [17], the multiphase interleaved converter and its basic working principle have been discussed with only the simulation and experiment comparison under idle state. This paper supplements the experimental content of the charging and discharging process. In this paper, the unbalanced cells in a battery pack are mathematically described in an energy exchange matrix, as do the switching states, which converts the battery energy transfer path into a linear algebraic problem. To clarify the feasibility of the strategy proposed in this paper, the converter for battery balancing is built in PSIM. Finally, a number of experiments verify that the proposed control strategy transfers battery energy to other cells in the stack quickly and flexible. In addition, analysis and explanation of the loss and efficiency of the converter under different numbers of batteries.

This paper is organized as follows. Section II presents the working principle of the flexible multiphase interleaved converter and its mathematical formula derivation. Simulation and PNGV model are demonstrated in Section III. Furthermore, Section III also presents experiment and result analysis. Come conclusions and future work directions are provided in Section IV.

II. Operating Principle and Design

A. Basic Design and Principle

A typical Buck-Boost circuit can only achieve unidirectional power transfer, while changing the original diode with a MOSFET transistor enables bidirectional energy exchange and a continuous current flow [18], [19]. The primary circuit of this equalization technology is shown in Fig. 1. The derived buck-boost converter makes power exchange from one overcharged cell to the others. Each equalizer is connected by an inductor between two cell subpacks. The two-cell equalization circuit is shown in Fig. 2. Each equalizer separates the cells into two sections, the upper section and the lower sections, whose energy can be mutually exchanged. This topology can also individually transfer the energy of any one cell to the other cells in a stack. When compared with a traditional equalization converter, it makes battery energy equalization more flexible and easier to expand. The expanded topology is shown in Fig. 3. Each equalizer in the multiphase interleaved converter divides the complete battery component into two adjacent continuous battery sub-packs. Furthermore, the equalization module that connected to the positive and negative terminals of the over-charged battery delivers the extra energy to all the other batteries in the pack.

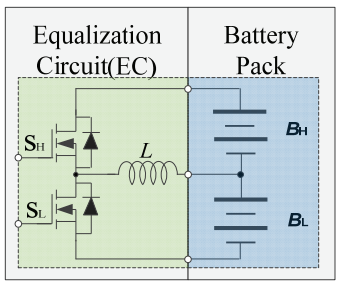

Fig. 1. Bidirectional buck-boost converter.

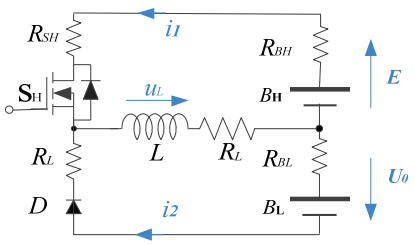

Fig. 2. Unidirectional buck-boost circuit principle (QBH>QBL).

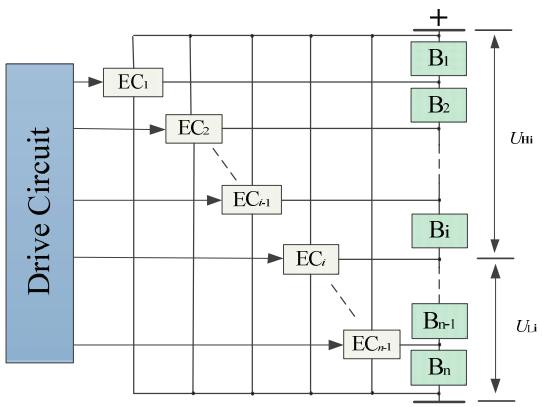

Fig. 3. Multilayer equalization circuit extended topology.

In the steady state, the integral of the applied inductor voltage must be zero.

$$\int_0^T u_L \mathrm{d}t = 0 \tag{1}$$

When S_H is in the on state, u_L=E. When S_H is in the off state, u_L=-u_0.

$$Et_{on} = U_0 t_{off} \tag{2}$$

$$U_0 = \frac{t_{on}}{t_{off}} E = \frac{t_{on}}{T - t_{on}} E = \frac{\alpha}{1-\alpha} E \tag{3}$$

B. Natural Spontaneous Balancing Control

The transistors of a converter work in a complementary driving mode, and their respective duty cycle is set by the formula of the input and the output voltage.

$$\alpha_i = U_{Hi} / \left(U_{Li} + U_{Hi}\right) \tag{4}$$

$$U_{Hi} = \sum_{x=1}^{i} U_{cellx} \tag{5}$$

$$U_{Li} = \sum_{x=i+1}^{n} U_{cellx} \tag{6}$$

$$R_{iINeq} = \sum_{x=1}^{i} R_{cellx} + R_{SHi} + R_{Li} \tag{7}$$

$$R_{iOUTeq} = \sum_{x=i+1}^{n} R_{cellx} + R_{SLi} + R_{Li} \tag{8}$$

$$\alpha_i U_{Li} - R_{iINeq} \alpha_i I_{Lm} = \left(1-\alpha_i\right) U_{Hi} + R_{iOUTeq} \left(1-\alpha_i\right) I_{Lm} \tag{9}$$

$$I_{Lm} = \frac{\alpha_i U_{Li} - \left(1-\alpha_i\right) U_{Hi}}{\alpha_i R_{iINeq} + \left(1-\alpha_i\right) R_{iOUTeq}} \tag{10}$$

The subscript ***i*** stands for the number of batteries in the input branch, i∈int [1; N-1], $\boldsymbol{U_{Hi}}$ is the input voltage of the cells, and $\boldsymbol{U_{Li}}$ stands for the output voltage of the cells. In constant duty cycle mode, the average voltage generated on one side of the inductor is equal to a portion of the voltage across the entire battery pack. If the voltage of the battery pack on both sides of the inductor is balanced, the potential at the other end of the inductor is also the same. That is to say, the two parts of the cells separated by the equalizer are offset by the effect of the inductance, and the balancing current is zero. If this is not the case, the current generated by the potential difference will flow through the inductor to balance the voltages of the two potentials. Table I shows the on-duty of each switch. In order to reduce the idle time of the equalizer, each switch operates in the complementary conduction mode.

C. Forced Active Balancing Control

To reduce repetitive consumption caused by energy cycling loss in the balancing process, a forced active equalization control is designed and demonstrated. The current flow is in the direction illustrated by the arrow. This converter performs an intuitive equalization control of the front cell and the rear cell in Fig. 4. In mode I, turning the switch S_{Li-1} on, the balancing current flows along the red arrow in Fig. 4(a). Then in mode II, turning off the switch S_{Li-1}, the balancing current flows along the red arrow in Fig. 4(a). Meanwhile, if the energy of an overcharged cell is delivered to the rest of the stacks, the above steps demands performed in a certain sequence, and the S_{Hi} needs to be turned on. In mode III, the balancing current flows along the blue arrow in Fig. 4(b). Then in mode IV, the switch S_{Hi} is turned off, and the balancing current flows along the red arrow in Fig. 4(b). Table II describes the status of the switches at each state. (0 for close; 1 for open).

TABLE I
DUTY CYCLE RATE OF THE EQUALIZATION CIRCUIT

S	EC(1)	EC(2)	…	EC(i)	…	EC(n-1)
S_H	(n-1)/n	(n-2)/n	…	(n-i)/n	…	1/n
S_L	1/n	2/n	…	i/n	…	(n-1)/n

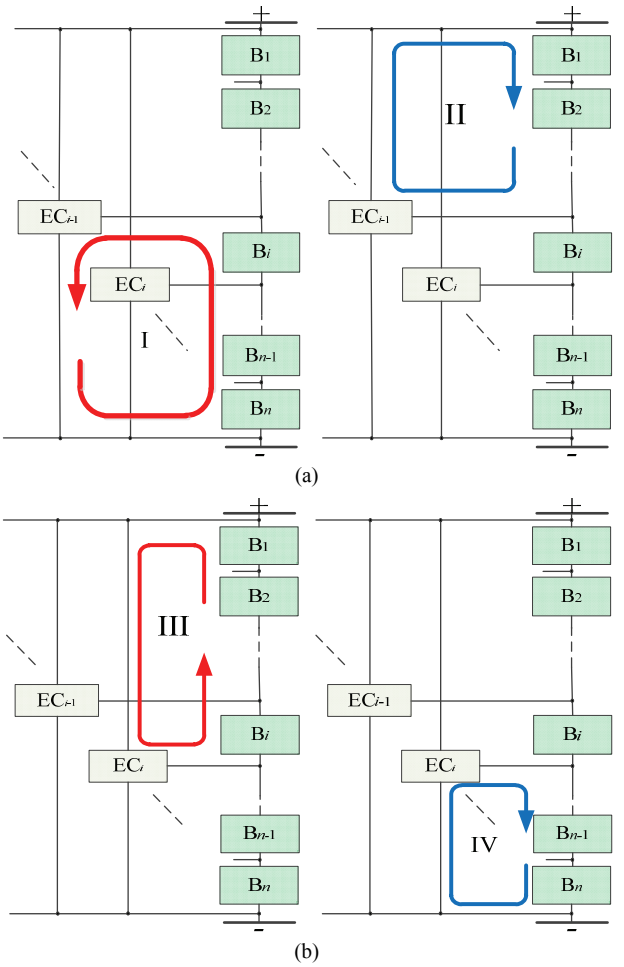

Fig. 4. Equilibrium current path of any unbalanced battery. (a) Current path in mode I and mode II. (b) Current path in mode III and mode IV.

The equilibrium of the battery string containing N cells is mathematically proved. The working principle is described as follows. Provided that B_i is overcharged, the extra-energy should be delivered to the other batteries. The extra-energy, given off from Bi to Bn, is temporarily stored by the inductor $\boldsymbol{L_{i-1}}$ where each of them contributes $\Delta\varepsilon_1$ in state I. Then

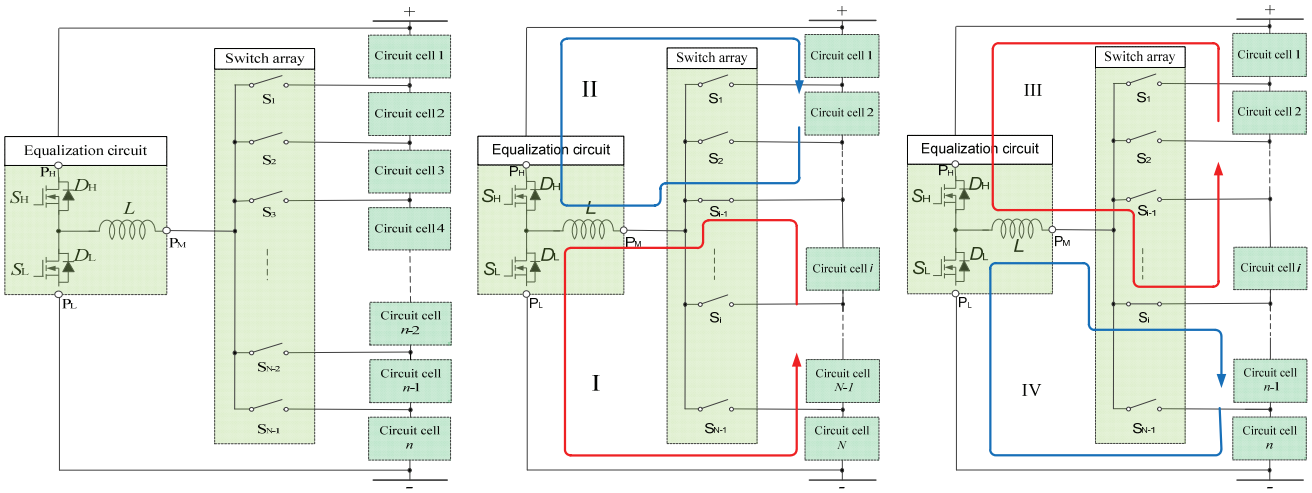

(a) (b) (c)

Fig. 5. Principle of the simplified equalization circuit. (a) Sharing equalization circuit. (b) When switch S_{i-1} is closed. (c) When switch S_i is closed.

TABLE II
SWITCHING STATE DURING EQUALIZATION

Switch	State I	State II	State III	State IV
$S_{H(i-1)}$	0	0	0	0
$S_{L(i-1)}$	1	0	0	0
$S_{H(i)}$	0	0	1	0
$S_{L(i)}$	0	0	0	0

inductor delivers this part of energy to the batteries from B_1 to B_{i-1} in state II. Then the energy, given off from B_1 to B_i, is temporarily stored by the inductor $\boldsymbol{L_i}$ where each of them contributes $\Delta\varepsilon_2$ in state III. The inductor delivers this energy to the batteries from B_{i+1} to B_n in state IV. The difference energy between the battery B_i and that of the whole battery stack is defined as Q_i. The amount of energy transferred from each one in the cells is described by equations (11) and (12).

$$(n-i+1)\Delta\varepsilon_1/(i-1)-\Delta\varepsilon_2 = Q_i^{extra}/n \tag{11}$$

$$-\Delta\varepsilon_1+i\Delta\varepsilon_2/(n-i) = Q_i^{extra}/n \tag{12}$$

The simultaneous equations are solved:

$$\Delta\varepsilon_1 = (i-1)Q_i^{extra}/n \tag{13}$$

$$\Delta\varepsilon_2 = (n-i)Q_i^{extra}/n \tag{14}$$

The energy described by functions (4) and (5) can be reached with just two switches working. The structure is simple in design and convenient in terms of control. In addition, it is easily expandable to different scales of series battery packs. Because of the similarity in the topology of the N-phase converters, the topology is further simplified as shown in Fig. 5. The combination of an equalizer and a switch array replaces the original multiple equalizers, simplifying the circuit and reducing the number of components in the system.

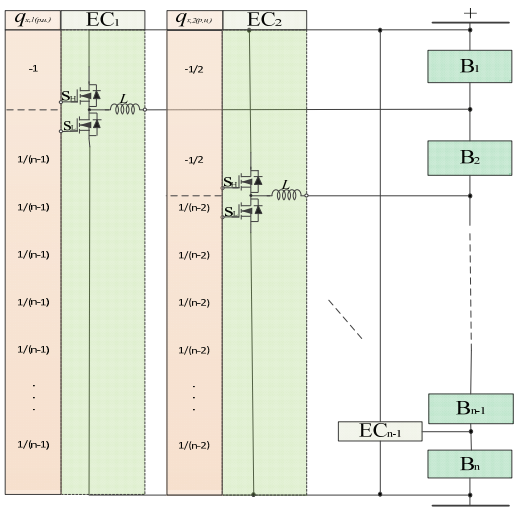

Fig. 6. Interlaced converter energy transfer diagram.

D. Overall Matrix Equalization Control

In general cell stacks, several cells are overcharged, while others are not. In addition, the two switching tubes in one equalizer have the opposite effect, and each equalization module only needs one switching to operate for equilibrium.

When the upper switch S_H in EC_1 is turned on, the battery B_1 transfers energy to the inductor $\boldsymbol{L}$. Subsequently, the inductor L divides this energy among the remaining cells, where all of the remaining of the n-1 batteries absorbs 1 / (n-1) part of energy. When the upper switch S_H of the equalization module EC_2 is turned on, both of the batteries B_1 and B_2 transfer 1/2 part of the energy to the inductor. Then the inductor releases energy to the remaining batteries, which means the remaining n-2 batteries absorb 1/(n-2) part of the energy. These equalization modules consist of 2n-2 switching tubes and n-1 inductors. To further reduce the number of components, the simplified circuit described above can be

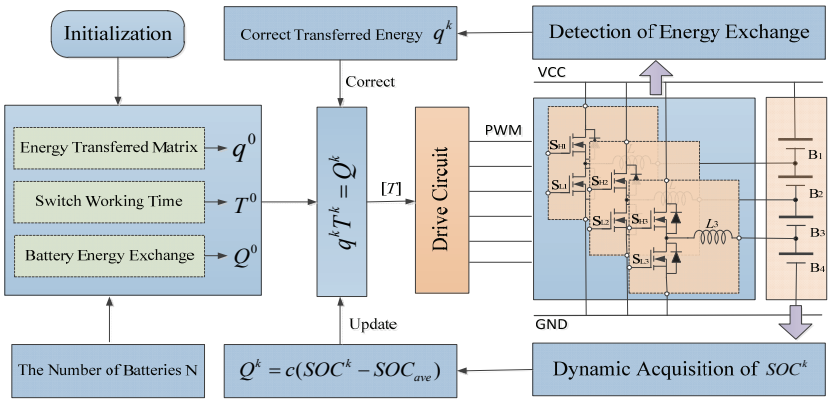

Fig. 7. Block diagram of the modulation scheme.

adopted. However, this is done at the expense of the loss of equalization time.

When compared with natural equalization, the current hybrid control equalization is larger. This is due to the fact that the hybrid control equalization electromotive force is provided by the overcharged partial battery pack. However, the natural equalization electromotive force is provided by the energy difference between the two-part. When compared with forced equalization, the equalization current is the same. In the forced equalization control, the extra-energy is transferred one by one, which causes the upper and lower switchings of the equalization to serve the energy equalization process of different batteries. Up to one switching tube in the equalization module is working in hybrid equalization, which avoids the energy transfer effect from the repeated operation of the upper and lower switching tubes.

Initially, the SOC of all the batteries is measured to calculate SOC_{ave}. Equ. (15) gives the calculation method of the average power of the battery. Then the energy transfer matrix of the equalization module is multiplied by the time t to obtain the energy exchange amount after all of the batteries reach equilibrium, as shown in Equ. (16). The time matrix is solved by MATLAB to find the working time of each switch. A single-chip microcomputer is required to control the switch tube according to the time matrix reducing the energy circulation. This in turn, improves the working efficiency of the equalization circuit. The specific solution is introduced in the appendix.

$$Q_{\bar{B}} = \frac{\sum_{i=1}^{n} Q_{B_i}}{n} \tag{15}$$

$$\sum_{j=1}^{2n-2} q_j t_j = \begin{bmatrix} Q_{B_1} - Q_{\bar{B}} \\ Q_{B_2} - Q_{\bar{B}} \\ \vdots \\ Q_{B_i} - Q_{\bar{B}} \\ \vdots \\ Q_{B_{n-1}} - Q_{\bar{B}} \\ Q_{B_n} - Q_{\bar{B}} \end{bmatrix} \tag{16}$$

A block diagram of this system is shown in Fig. 7. This system was adopted to implement the charge balancing schemes.

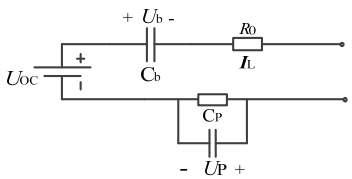

Fig. 8. PNGV equivalent circuit model.

During the equalization process, the SOC is updated dynamically to be applied to the energy matrix. The latest solution is used to drive the equalization module again.

III. Simulation and Experimental Results Analysis

A. Battery Modelling and Parameters Identification

The PNGV model is shown in Fig. 8 [20]-[22]. It has a higher precision and a more accurate description of the transient response process of a battery than the Thevenin model or the R_{int} model. In this model, U_{OC} stands for the ideal voltage source which is the same as the open circuit voltage of the battery; R_0 is the internal resistance of the battery; R_P is the polarization resistance; C_P is the polarization capacitance; I_P is the current on the polarization resistance; and C_B is the capacitance that describes the change in the open circuit voltage that accumulates.

Available for the circuit diagrams C_B and C_P:

$$C_b \frac{\mathrm{d}U_b}{\mathrm{d}t} = I_L \tag{17}$$

$$C_p \frac{\mathrm{d}U_P}{\mathrm{d}t} = I_L - \frac{U_P}{R_P} \tag{18}$$

According to Kirchhoff's voltage law, the open circuit voltage U_{OC} can be:

$$U_{OC} = U_b + U_P + I_L R_0 + U_L \tag{19}$$

The equation of the state for building the PNGV model with the two capacitor voltages U_B and U_P is:

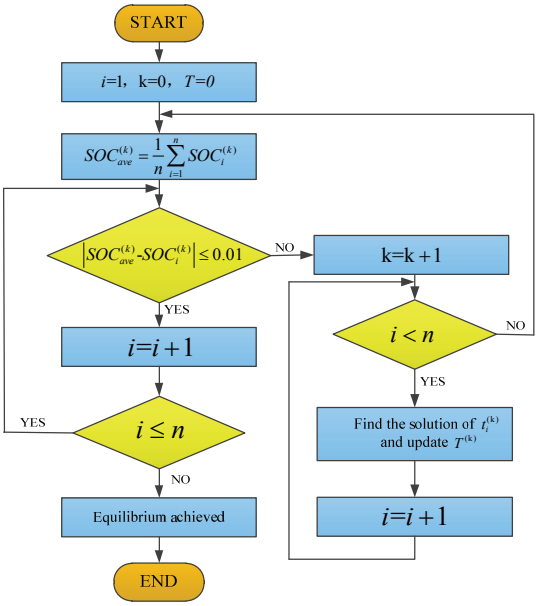

Fig. 9. Block diagram of the system.

$$\begin{cases}\begin{bmatrix}U_b\\U_P\end{bmatrix}=\begin{pmatrix}0 & 0\\0 & -\frac{1}{C_P R_P}\end{pmatrix}\begin{bmatrix}U_b\\U_P\end{bmatrix}+\begin{bmatrix}\frac{1}{C_b}\\\frac{1}{C_P}\end{bmatrix}[I_L]\\U_L=[-1,-1]\begin{bmatrix}U_b\\U_P\end{bmatrix}+[-R_0][I_L]+[U_{OC}]\end{cases} \quad (20)$$

Where the two capacitor voltages act as state variables, and the battery terminal voltage acts as the output variable. The SOC, the criterion for achieving equalization, is not a directly measurable physical quantity. It is estimated by collecting the port voltage U_{OC} and the port current I_L, which are both measurable electrical parameters. A flow diagram of the system is depicted, as shown in Fig. 9.

B. Analysis of Simulation Results

The balancing circuit and its working principle mentioned above, with the natural equalization control and the overall matrix equalization control, is proved respectively. A simulation model is built in PSIM in this section. This model includes a PNGV model and an experimental platform for four lithium-ion batteries.

In the experimental design, B_2 was initially overcharged (i=2, U_{B2}=4V, U_{B1}=U_{B3}=U_{B4}=3.6V). The working principle of balancing the energy of B_2 and the other cells is simulated and confirmed. The equalization circuit containing two batteries is equipped with one equalizer. Simulation experiments are demonstrated under both the natural equalization and overall matrix equalization control. The waveforms of the drive signal, current on inductor and voltage of battery in the four operating modes of the circuit simulation are shown in Fig. 10.

The switch S_{H2} has a conduction duty ratio of 50%. When the switch S_{H2} is turned on, B_1 and B_2 transfer energy to the inductor. When the switch S_{H2} is turned off, the inductor releases energy to B_3 and B_4. The switch S_{L1} has a conduction

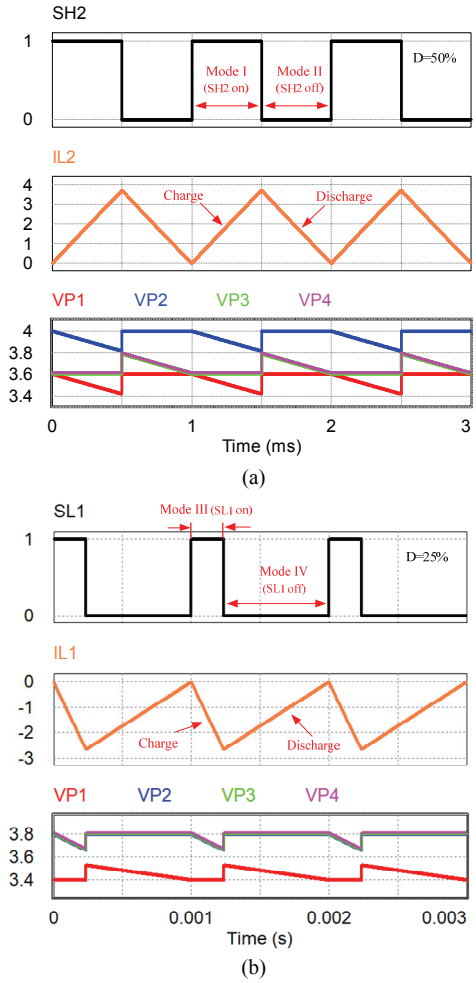

Fig. 10. Dynamic voltage waveform in forced equilibrium. (a) Key operation waveform in modes I and II. (b) Key operation waveform in modes III and IV.

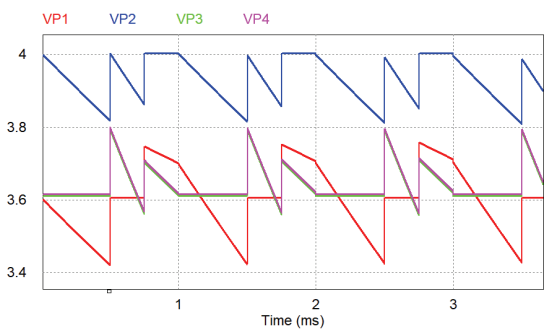

Fig. 11. Dynamic voltage waveform with the HNFABC.

duty ratio of one quarter. When the switch S_{L1} is turned on, B_2, B_3 and B_4 transfer energy to the inductor. When the switch S_{L1} is turned off, the inductor releases energy to B_1.

In the HNFABC, considering the overall balance of the battery pack, the working hours of each group of switch tubes are obtained based on the energy variation matrix. The drive circuit controls the operation of each switch tube. In any group of switch tubes, at most one switch is working to achieve balance, which avoids repeated energy exchange.

TABLE III
SIMULATION AND EXPERIMENTAL SPECIFICATIONS

Item	Description
Microprocessor	STM32F103
Cell parameter	4.2V,1AH
Inductance value	100uH
Switch model	IRF530N
Frequency	10kHz
Duty cycle of S_{H2}	50.0%
Duty cycle of S_{L1}	25.0%
The initial state of B1	4.0V
The initial state of B2	3.6V
The initial state of B3	3.6V
The initial state of B4	3.6V

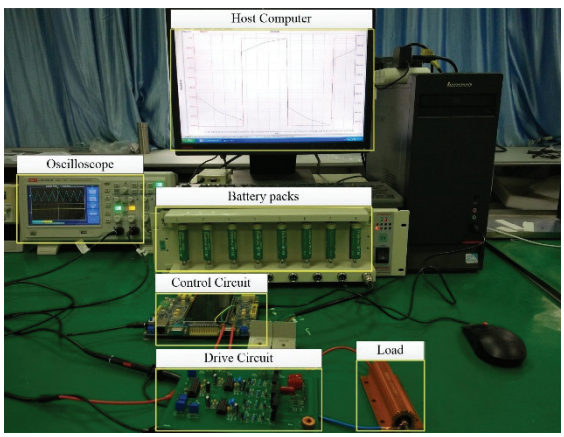

Fig. 12. Experimental platform for testing.

C. The Analysis of Experiment Results

Simulation and experimental results prove the feasibility of the design proposed in this paper. The component parameters in the experiment are shown in Table III.

An experimental platform has been built in the laboratory to verify the feasibility of the proposed method as shown in Fig. 12. In order to make the effect more intuitive, B_1 is overcharged in the experiment. The goal is to transfer the excess energy of B_1 to B_2, B_3 and B_4 equally. In the equalization of four battery packs, the three equalizer modules include six switch tubes. The power transfer matrix of each switch tube is shown in equation (21).

$$q_{i,j}(p.u.)=\begin{bmatrix} -1 & -\frac{1}{2} & -\frac{1}{3} \\ -\frac{1}{3} & -\frac{1}{2} & -\frac{1}{3} \\ -\frac{1}{3} & \frac{1}{2} & -\frac{1}{3} \\ -\frac{1}{3} & \frac{1}{2} & 1 \end{bmatrix} \tag{21}$$

To obtain the specific element value of the matrix:

$$I=\frac{DU}{Lf} \tag{22}$$

where $\boldsymbol{D}$ is the duty cycle of the switch $\mathbf{S_H}$; $\boldsymbol{U}$ is the voltage of the battery packs; $\boldsymbol{L}$ is the value of the inductor; and $\boldsymbol{f}$ is the

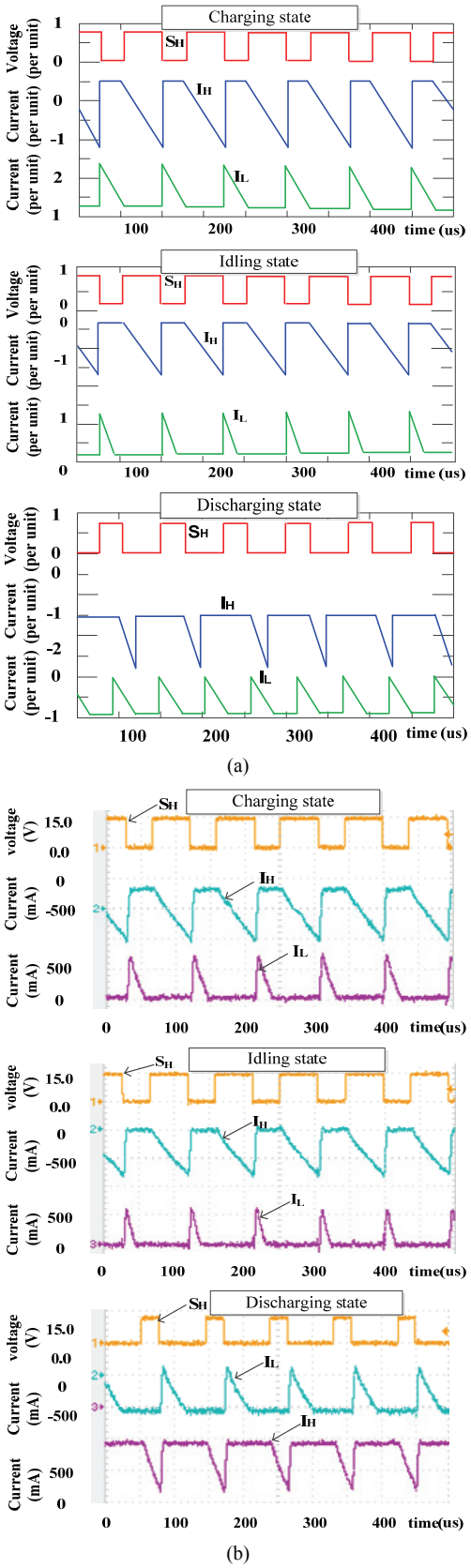

Fig. 13. Key waveforms of the simulation and experiment. (a) Simulation waveforms in the charging, idling and discharging states. (b) Experimental waveforms in the charging, idling and discharging state.

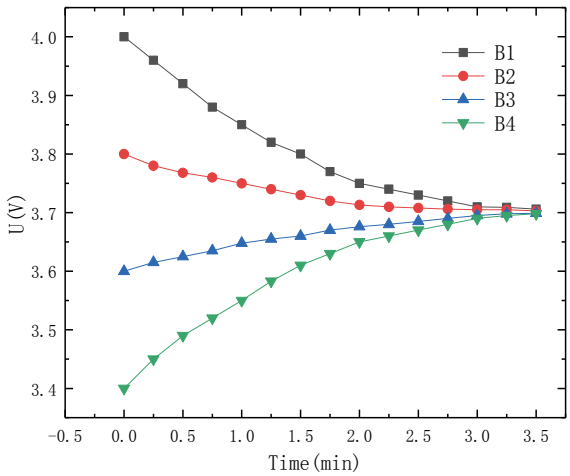

Fig. 14. Experimental results for natural active balancing control.

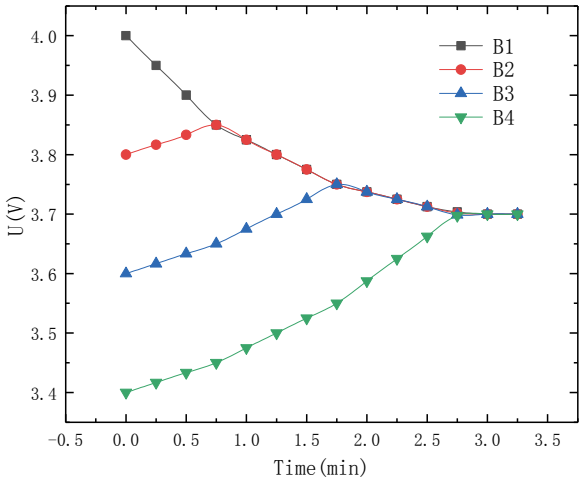

Fig. 15. Experimental results for forced active balancing control.

frequency of the PWM. Calculating the energy storage according to the inductance yields the value of $\boldsymbol{q}$ in the matrix:

$$q_{(1,1)}=\int_0^I Lidi=\frac{1}{2}LI^2 \tag{23}$$

In order to verify the above design, the simulation and experiment under charging, discharging and idle state are respectively shown in Fig. 13. The waveform of the experimental result has a good consistency with the waveform of the simulation result.

Simulation and experiment use the same component parameters and compare as much as possible in a similar condition. In the state of charging, discharging and idle, the average value of I_H is smaller than the average value of I_L, so that the energy of battery B_H is transferred to battery B_L. It's clearly arrived at that according to the state of the switch in the simulation, the current waveform in the experiment is in good consistent with the waveform in the simulation.

D. Results Analysis

Four series battery packs set with the same parameters are balanced and compared under the following three control strategies.

1) Working Condition One: Natural Active Balancing Control. In the experiment, the average voltage of the battery was 3.7V, and the battery voltage gradient was set to 0.2V. The following working conditions are the same as above.

In the experiment, the battery voltage was collected every fifteen seconds, and the voltage change curve was plotted as shown in Fig. 14. It is concluded that the voltage does not cross the average value during the charge or discharge states, in which there is no repeated charge and discharge state. However, when the equalization is working, the voltage difference of the battery decreases and the energy transferred in one cycle is also reduced, which slows down the equalization speed.

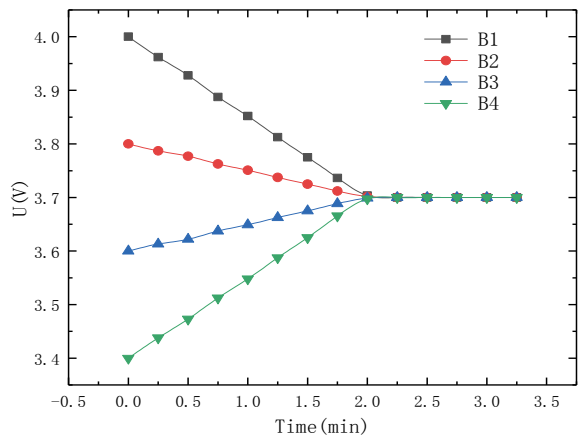

Fig. 16. Experimental results for hybrid balancing control.

2) Working Condition Two: Forced Active Balancing control. As shown in Fig. 15, forced active balancing slightly increases the speed of equalization. However, the batteries are being repeatedly charged and discharged (both B_2 and B_3 are charged and then discharged), which accelerates battery aging.

3) Working Condition Three: Hybrid Naturally and Forced Active Balancing Control. As shown in Fig. 16, the equilibrium speed is constant without slowing down. The testing object is always in the state of charging or discharging (B_1 and B_2 are discharged, B_3 and B_4 are charged), without repeated charging and discharging, which reduces the damage to the battery.

Compared with traditional circuits, the flexible interlaced converter has fewer components and lower voltage stress, which reduces the cost of the system and improves system stability. Deep analyses of the efficiency and power loss of the systems were performed as shown in Fig. 17.

When the number of batteries increases, the energy and circuit losses transferred by the equalizer increase. However, the efficiency of the system increases slightly. This means that when the number of batteries is small, the advantages of

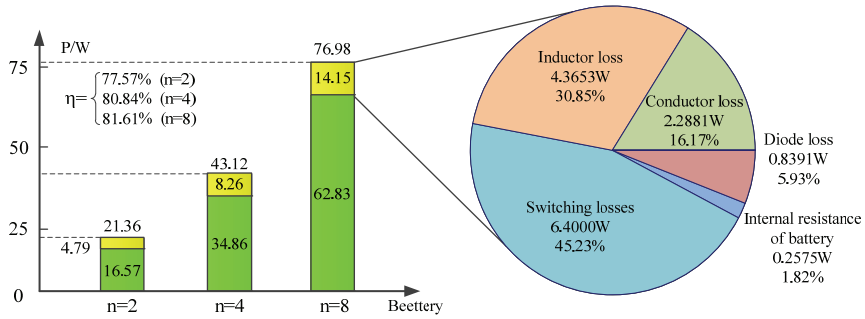

Fig. 17. Power loss distributions in the experiment.

TABLE IV
TYPICAL EQUALIZATION DEVICE COMPARISON

Topology	Component		Voltage stress		Inductor	transformer
	#S	#D	#S	#D		
#1	0		0		0	0
#2	1		N		N*V	V
#3	N		N		V	V
#4	2N-2		0		V	V

#1: flying-capacitor equalization topology; #2: multi- output winding transformer centralized equalization structure; #3: buck-boost centralized equalization structure; #4: flexible interlaced converter structure; #S: switch; #D: diode.

the topology and its control method are not very obvious. However, with the further expansion of the equalization converter, the design reduces the characteristics of the battery so that it is repeatedly charged and discharged more prominently. By analyzing the energy loss of each part of the eight-cell series equalization, the main power loss of the system can be obtained by the switching and the inductor. Meanwhile, the application of low on-resistance SiC devices significantly reduces system losses in the future.

IV. CONCLUSIONS

In this paper the NHFABC strategy was proposed for a flexible battery energy balancing converter based on the PNGV model. The obtained analysis of experimental results concluded that the multiphase equalization converter with overall matrix equalization control achieved energy balancing, prolonged the service life of the battery stack, meanwhile reduced the energy loss in the equilibrium process. The main merit of this topology is that only half of the switches need to work to deliver excess power from the overcharged batteries to the other batteries, which avoids battery damage caused by repeated charge and discharge processes. According to the simulation results, this control strategy was shown to be more effective in the utilization of switches to enhance control performance when compared with traditional equalization control.

This paper presents a flexible interleaved converter and its control proposed which are suitable for the bidirectional power transfer applications in new energy electric vehicles. Future research will investigate the association between equalization efficiency and the coupling effect of inductors while using SiC devices. They will comprehensively analyze practical engineering problems, and reduce the power loss and volume of the passive devices.

APPENDIX

The source code for solving the time matrix using MATLAB is as follows:

```
function [S_H, S_P] = solveLS(A,b)
% Input parameter A: coefficient matrix
% Input parameter B:Ax=b Constant term column vector b
% S_H : Basic solution system of homogeneous linear equations
% S_P : Special solutions of nonhomogeneous linear equations
if size(A,1) ~= length(b) %size(A,1) Find the number of rows in the matrix
    error(' Input data error ! ');
    return;
else
    B = [A,b];   % Augmented matrix
    rank_A = rank(A);     % Find the rank of the coefficient matrix
    rank_B = rank(B);     % Find the rank of the augmented matrix
    if rank_A ~= rank_B % No solution
        disp(' Linear equations have no solution ! ');
        S_H = [];
        S_P = [];
    else if rank_B == size(A,2) % If Rank of augmented matrix = Unknown quantity
        %size(A,2) Find the number of columns in the matrix
        disp(' Linear equations have a unique solution ! ');
        S_P = A\b;   % Figure out unique solution
        S_H = [];
    else
        disp(' Linear equations have infinite solutions!');
```

```
            S_H = null(A,'r'); % Find the basic solution system of homogeneous equations
            S_P = A\b;
    % special solutions of nonhomogeneous equations
            end
        end
    end
```

Set the number of batteries in the battery pack n=4. Input energy transfer matrix A and power change amount matrix b.

```
A=[-3 -2 -1 3 2 1;1 -2 -1 -1 2 1;1 2 -1 -1 -2 1;1 2 3 -1 -2 -3];
b=[0 -1 1 0]';format rat;
[S_H, S_P]=solve LS(A,b)
```

Get output t=[-1/4 1/2 -1/4 0 0 0] Considering that the on-time of the switch is non-negative, the actual on-time array t is [0 1/2 0 1/4 0 1/4].

REFERENCES

[1] K. Yang and A. Walid, "Outage-storage tradeoff in frequency regulation for smart grid with renewables," *IEEE Trans. Smart Grid*, Vol. 4, No. 1, pp. 245-252, Mar. 2013.

[2] T. Masuta and A. Yokoyama, "Supplementary load frequency control by use of a number of both electric vehicles and heat pump water heaters," *IEEE Trans. Smart Grid*, Vol. 3, No. 3, pp. 1253-1262, Sep. 2012.

[3] J. J. Escudero-Garzas, A. Garcia-Armada, and G. Seco-Granados, "Fair design of plug-in electric vehicles aggregator for V2G regulation," *IEEE Trans. Veh. Technol.,* Vol. 61, No. 8, pp. 3406-3419, Oct. 2012.

[4] A. Khaligh and Z. Li, "Battery, ultracapacitor, fuel cell, and hybrid energy storage systems for electric, hybrid electric, fuel cell, and plug-in hybrid electric vehicles: State of the art," *IEEE Trans. Veh. Technol.*, Vol. 59, No. 6, pp. 2806-2814, Jul. 2010.

[5] J. C. Gomez and M. M. Morcos, "Impact of EV battery chargers on the power quality of distribution systems," *IEEE Power Eng. Rev.*, Vol. 18, No. 3, pp. 975-981, Jul. 2003.

[6] S. Han, S. Han, and K. Sezaki, "Development of an optimal vehicle-to-grid aggregator for frequency regulation," *IEEE Trans. Smart Grid*, Vol.1, No. 1, pp. 65-72, Jun. 2010.

[7] E. Inoa and J. Wang, "PHEV charging strategies for maximized energy saving," *IEEE Trans. Veh. Technol.*, Vol. 60, No. 7, pp. 2978-2986, Sep. 2011.

[8] B. Zhu, Q. Zeng, Y. Chen, Y. Zhao, and S. Liu, "A dual-input high step-up DC/DC converter with ZVT auxiliary circuit," *IEEE Trans. Energy Convers.*, Vol. 34, No. 1, pp. 161-169, Mar. 2019.

[9] S.-W. Lee, K.-M. Lee, and Y.-G. Choi, "Modularized design of active charge equalizer for Li-Ion battery pack," *IEEE Trans. Ind. Electron.*, Vol. 65, No.11, pp. 8697-8706, Nov. 2018.

[10] A. M. Imtiaz and F. H. Khan, "Time shared flyback converter" based regenerative cell balancing technique for series connected Li-Ion battery strings," *IEEE Trans. Power Electron.,* Vol. 28, No. 12 pp. 5960-5975, Dec. 2013.

[11] C.-S. Lim, K.-J. Lee, and N.-J. Ku, "A modularized equalization method based on magnetizing energy for a series-connected lithium-ion battery string," *IEEE Trans. Power Electron.,* Vol. 29, No. 4, pp. 1791-1799, Apr.2014.

[12] W. Huang and J. A. Abu Qahouq, "Energy sharing control scheme for state-of-charge balancing of distributed battery energy storage system," *IEEE Trans. Ind. Electron.*, Vol.62, No.5, pp.2764-2776, May 2015.

[13] Y. Wei, Y. Li, B. Cao, and B. Zhu "Research on power equalization of lithium-ion batteries with less-loss buck chopper," *Trans. China Electrotechn. Soc.*, Vol. 33, No.11, pp.2575-2583, Nov.2017.

[14] S. Dai, Y. Wei, X. Zhang, and Z. Shan, "Low-loss power equalization technique for Li-ion battery," *Battery Bimonthly*, Vol. 48, No. 3, pp. 175-178, Jun. 2018.

[15] J. Li and J. Jiang, "Active capacitor voltage balancing methods based on dynamic model for five-level nested neutral point piloted converter," *IEEE Trans. Power Electron.*, Vol. 33, No.8, pp.6567-6581, Aug.2018.

[16] D. Yang, W. Ning, and Y. Li, "Natural frame control of single-phase cascaded H-bridge multilevel converter based on fictive-phases construction," *IEEE Trans. Ind. Electron.*, Vol. 65, No. 5, pp. 3848-3857, May 2018.

[17] Y. Wei, S. Dai, J. Wang, Z. Shan, and J. Min, "Hybrid natural and forced active balancing control of battery packs state of charge based on partnership for a new generation of vehicles," *J. Electr. Comput. Eng.*, Vol. 2018, 2018.

[18] F. Mestrallet, L. Kerachev, and J.-C. Crebier, "Multiphase interleaved converter for lithium battery active balancing," *IEEE Trans. Power Electron.*, Vol. 29, No. 6, pp. 2874-2881, Jun. 2014.

[19] V. Yuhimenko, G. Geula, and G. Agranovich, "Average modeling and performance analysis of voltage sensorless active supercapacitor balancer with peak current protection," *IEEE Trans. Power Electron.*, Vol. 32, No. 2, pp. 1570-1578, Feb. 2017.

[20] C. Liu, W. Liu, and L. Wang "A new method of modeling and state of charge estimation of the battery," *J. Power Sources*, Vol. 320, pp. 1-12, Jul. 2016.

[21] X. Liu, W. Li, and A. Zhou, "PNGV equivalent circuit model and SOC estimation algorithm for lithium battery pack adopted in AGV vehicle," *IEEE ACCESS*, Vol.6 pp. 23639-23647, 2018.

[22] X. Hu, R. Xiong, and B. Egardt, "Model-based dynamic power assessment of lithium-ion batteries considering different operating conditions," *IEEE Trans. Ind. Informat.*, Vol. 10, No. 3, pp. 1948-1959, Aug. 2014.

Shuailong Dai was born in Xiangyang, China, in 1996. He received his B.S. degree in Electrical Engineering from the School of Electrical Engineering and New Energy, China Three Gorges University, Yichang, China, in 2018, where he is presently working towards his M.S. degree in the School of Electrical Engineering and New Energy. His current research interests include bidirectional DC/DC converters, equilibrium circuit systems, energy internet and distributed energy storage.

Jiayu Wang was born in Xiangyang, China, in 1998. He is presently working towards his B.S. degree in Electrical Engineering and Automation at the China Three Gorges University, Yichang, China. His current research interests include circuit modeling, battery energy equalization, and the application of more advanced algorithms on energy equalization circuit control.

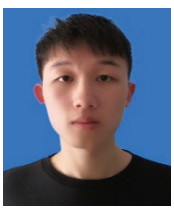

Teng Li was born in Hebei Province, China, in 2000. He is presently working towards his B.S. degree in the Department of Automation, China Three Gorges university. His current research interests include power electronics, equalization technology, and energy storage systems.

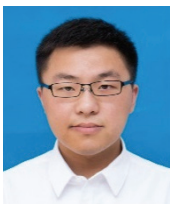

Zhifei Shan was born in Zhejiang Province, China. He received his B.S. degree in the Collage of Science and Technology, China Three Gorges University, Yichang, China, where he is presently working towards his M.S. degree in the School of Electrical Engineering and New Energy. His current research interests include equilibrium circuit systems, energy internet, and smartgrid.

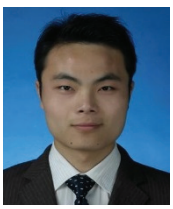

Yewen Wei was born in Hunan Province, China. He received his B.S. degree in Measurement and Control Technology for Instruments from Xiangtan University, Xiangtan, China, in 2008. He is presently working towards his Ph.D. degree in the School of Electric Power, South China University of Technology, Guangzhou, China. Since 2016, he has been working at the China Three Gorges University, Yichang, China. His current research interests include power electronic converters, renewable energy systems, reactive power control, Magnetic Energy Recovery Switch (MERS), and FACTS devices.